HHS Public Access

Author manuscript

Fertil Steril. Author manuscript; available in PMC 2020 August 01.

Published in final edited form as:

Fertil Steril. 2019 August ; 112(2): 387–396.e3. doi:10.1016/j.fertnstert.2019.04.001.

Body mass index in relation to extracellular vesicle linked microRNAs in human follicular fluid

Rosie M Martinez, ScD, MPH[1], **Andrea A. Baccarelli, MD, PhD**[2], **Liming Liang, PhD**[3], **Laura Dioni, PhD**[4], **Abdallah Mansur, MS**[5], **Michal Adir, BsC**[5], **Valentina Bollati, MD**[4], **Catherine Racowsky, PhD**[6], **Russ Hauser, MD, ScD**[7], **Ronit Machtinger, MD**[5,*]

[1]Department of Environmental Health, Harvard T.H. Chan School of Public Health, Boston, Massachusetts 02115, USA; and at the Laboratory of Precision Environmental Biosciences, Department of Environmental Health Sciences, Columbia Mailman School of Public Health, New York, New York 10032, USA

[2]Laboratory of Precision Environmental Biosciences, Department of Environmental Health Sciences, Columbia Mailman School of Public Health, New York, New York 10032, USA

[3]Department of Biostatistics, Harvard T.H. Chan School of Public Health, Boston, Massachusetts 02115, USA

[4]EPIGET - Epidemiology, Epigenetics and Toxicology Lab, Department of Clinical Sciences and Community Health, University of Milan, 20122 Milano, Italy

[5]Department of Obstetrics and Gynecology, Sheba Medical Center, Ramat-Gan, 52561 and Sackler School of Medicine, Tel-Aviv University, Israel.

[6]Department of Obstetrics, Gynecology and Reproductive Biology, Brigham and Women's Hospital, Harvard Medical School, Boston, Massachusetts 02115, USA

[7]Department of Environmental Health, Harvard T.H. Chan School of Public Health, Boston, Massachusetts 02115, USA

Abstract

Objective: To study whether increased body mass index is associated with altered expression of extracellular vesicle microRNAs (EV-linked miRNAs) in human follicular fluid.

Design: A cross-sectional study

Setting: Tertiary, university-affiliated center

Patients: One hundred and thirty-three women undergoing in vitro fertilization (IVF) were recruited between January 2014 and August 2016.

[*]address of corresponding author: Ronit.Machtinger@sheba.health.gov.il.

Conflict of interest:
The authors have no conflicts of interest to declare.

Interventions: None

Main Outcome Measures: EV-linked miRNAs were isolated from follicular fluid and their expression profiles were measured using the TaqMan Open Array® Human miRNA panel. EV-linked miRNAs were globally normalized and inverse-normal transformed. Associations between BMI and EV-linked miRNA outcomes were analyzed using multi-variate linear regression and principal component analysis.

Result(s): Eighteen EV-linked miRNAs were associated with an increase in BMI after adjusting for age, ethnicity, smoking status and batch effects. Hsa-miR-328 remained significant after false-discovery rate adjustments. Principal component analyses identified the first principal component to account for 40% of the variation in our EV-linked miRNA dataset and adjusted linear regression found the first principal component was significantly associated with BMI after multiple testing adjustments. Using Kyoto Encyclopedia of Genes and Genomes enrichment analyses, we predicted gene targets of EV-linked miRNA *in silico* and identified PI3K-Akt signaling, ECM-receptor interaction, focal adhesion, FoxO signaling, and oocyte meiosis pathways.

Conclusions: These results show that a one-unit increase in BMI is associated with altered follicular fluid expression of EV-linked miRNAs that may influence follicular and oocyte developmental pathways. Our findings provide potential insight into a mechanistic explanation for the reduced fertility rates associated with increased BMI.

Capsule:

An increase in BMI was associated with EV-linked miRNA expression in human follicular fluid.

Keywords

IVF; microRNAs; extracellular vesicles; BMI

Introduction:

Human infertility is influenced by a broad range of physical, hormonal, genetic and environmental stressors (1). Despite enormous advances in the technical aspects of IVF, the success rates of the procedure remain relatively low. Whereas much has been published about non-modifiable factors associated with outcomes of IVF such as female age, fertility diagnosis, and ovarian reserve, less attention has been devoted to modifiable behavioral risk factors, such as body mass index (BMI) that may influence IVF outcomes (2-4).

Studies have shown that an increased BMI and obesity alter follicular development, oocyte maturation, and reduced numbers of oocytes retrieved (5-9). Women with a BMI ≥ 25 kg/m^2 undergoing IVF have a significantly reduced chance of a clinical pregnancy compared to women with BMI < 25 kg/m^2 (10-12). Despite the ample epidemiologic evidence, the molecular mechanisms underlying how increased BMI contributes to infertility are still unknown.

The ovarian follicle houses the oocyte itself and as it matures, cellular differentiation occurs, creating cellular layers of thecal, mural granulosa, and cumulus cells. Theca and granulosa cells create the membrane of the follicle itself, while cumulus cells encapsulate the oocyte

(13, 14). Follicular fluid is a crucial microenvironment for the developing oocytes, containing hormones, metabolites, ions, proteins, and various biological structures including non-coding RNAs and extracellular vesicles (EVs) (14-21). EVs, membrane enclosed structures (22), have been identified as a means for intercellular communication between the granulosa cells and oocyte in the follicular fluid (15). They are nanosized (30-700 nm in diameter) and can contain numerous molecules involved in cell signaling and cell to cell communication, including microRNAs, which are short non-coding RNA molecules (approximately 22 nucleotides long) (23). MicroRNAs are short, non-coding RNA molecules that can post-transcriptionally regulate gene expression (24-26) and can be free-floating or packaged in extracellular vesicles (EV-linked miRNAs). Extracellular vesicles (exosomes, micro-vesicles, and other membrane-bound vesicles) have been detected in almost every biofluid, including follicular fluid (22), and can act as a vehicle carrying proteins, messenger RNAs (mRNAs), and microRNAs (miRNAs) (27). These extracellular vesicle linked microRNAs (EV-linked miRNAs) can be encapsulated within the EV itself, but also associated with the EV extracellularly (28). These EV-linked miRNAs can influence gene expression and may be important for follicular signaling (15, 29, 30).

Several studies to date have reported possible associations between BMI and EV-linked miRNA profiles either in adipocytes or serum linking some of these EV-linked miRNAs with pathways of inflammation and insulin resistance (31-34). To the best of our knowledge, no study has examined associations between BMI and EV-linked miRNAs found in follicular fluid. Investigating EV-linked miRNAs in follicular fluid might help elucidate the mechanisms and pathways by which these modified risk factors that can impact fertility. Therefore, this study was aimed to investigate the effects of BMI with EV-linked miRNA expression isolated from follicular fluid in women undergoing IVF treatment.

Materials & Methods:

Ethics

This study was approved by Sheba Medical Center IRB in accordance with the Declaration of Helsinki (35). All participants provided written informed consent upon enrollment.

Study Population:

Between January 2014 and August 2016, women undergoing IVF were recruited in a tertiary care university-affiliated hospital. Eligibility criteria were women aged 19 to 38 years old, undergoing their 1st to 6th IVF attempt with a basal FSH less than 10 IU. To avoid potential confounding by the stimulation regimen or fertility diagnosis, we enrolled only women that were treated using GnRH antagonist protocol as well as women undergoing IVF due to unexplained infertility, mild male factors or women undergoing IVF for pre-gestational diagnosis of autosomal recessive disorders. We excluded those with a diagnosis of polycystic ovarian syndrome (PCOS), endometriosis or poor responders according to Bologna criteria (36) which might impair oocyte quality. All women contributed a single IVF cycle.

Exposure Assessment:

Participant's height and weight were measured at the beginning of the IVF cycle and were used to calculate body mass index (BMI, kg/m^2). Body mass index was calculated by dividing the weight (kg) of a person with the square of their height (m^2).

Outcome Assessment:

RNA extraction from follicular fluid: Follicular fluid (otherwise discarded material) was collected during oocyte retrieval from a single follicle ≥18 mm, per patient and centrifuged at 1500×g for 15 min. FF was aliquoted to 0.5 ml tubes So that the volumes of FF that were analyzed were equivalent among patients. Samples were pre-cleaned using a 0.80 um pore-size polyethersulfone filter (StericupRVP, Merck Millipore) to remove larger proteins and debris and aliquoted into 500 uL for immediate storage at −80°C (37). Only mature (MII) oocytes were examined for RNA analysis. Methods for RNA extraction from biological fluids have been previously described (38). In short, samples were thawed, centrifuged for 15 min at 1200 × g at room temperature and then centrifuged three times at 1000, 2000, and 3000 × g, respectively, for 15 min at 4°C Following this steps, samples were ultracentrifuged (Beckman Coulter Optima-MAX-XP) at 110,000 × g for 75 min at 4°C for the extraction of EV, as ultracentrifugation is considered the standard according to International Society for Extracellular Vesicle recommendations (28, 39). The pellets obtained were kept at −80°C until use. EV-linked miRNAs were extracted from the ultracentrifuged pellets using the miRNAeasy Kit and RNeasy CleanUp Kit per the manufacturer (Qiagen, Valencia, CA, USA). The final purified EV-linked miRNA-enriched RNA was eluted into 20 uL of RNAse-free water and stored at −80°C until further use. This protocol has been tested and samples have been examined by both Nanosight and Flow Cytometry for CD63 (an EV-specific marker) (results unpublished).

Expression analysis of EV-linked miRNAs in follicular fluid: We screened for 754 microRNAs using the TaqMan Open Array® system. We obtained 758 Crt values for each follicular fluid sample, which included 754 unique miRNAs and four internal controls (ath-miR159a, RNU48, RNU44 and U6). Methods of Real-Time Quantitative Polymerase Chain Reaction (RT-qPCR) for screening EV-linked miRNAs using the microRNA array in biological fluids are published elsewhere (38). QuantStudio™ 12K Flex is a fixed-content panel containing validated human TaqMan® MicroRNA Assays derived from Sanger miRBase release v.14. All 754 assays have been functionally validated with miRNA artificial templates. The panel is specifically designed to provide specificity for only the mature miRNA targets. TaqMan MicroRNA Assays (spotted in the panel) incorporate a target-specific stem–loop reverse transcription primer allowing to work despite the short length of mature miRNAs (~22 nucleotides) which prohibits conventional design of primers. Briefly, we prepared 3.3 uL of each RNA sample and then reverse-transcribed to cDNA (complementary DNA) and pre-amplified. Pre-amplified samples were mixed with the TaqMan Open Array® Real Time PCR Master Mix (Life Technologies, Foster City, CA) and loaded onto a TaqMan™ OpenArray® Human miRNA panel with the QuantStudio™ AccuFill System Robot (Life Technologies, Foster City, CA). RT-qPCR was performed on the QuantStudio™ 12K Flex Real-Time PCR System with the OpenArray® Platform [QS12KFLEX] (Life Technologies, Carlsbad, CA) according to the manufacturer's

instructions. Expression levels were calculated in relative cycle threshold values (Crt), estimating the amplification cycle at which the fluorescence levels for each of the analyzed EV-linked miRNAs exceed the background fluorescence threshold (40).

Covariate Assessment:

Participant's age, number of previous IVF attempts, and number of oocytes retrieved at the start of IVF cycle were extracted from participant's medical charts. Cigarette smoking status was determined by a questionnaire in which participants were asked about cigarette smoking history and intensity. Smoking status was categorized as never smokers, former smokers, and current smokers. Those who self-identified as former smokers stopped smoking prior to the beginning of their IVF cycle. Follicular fluid samples were analyzed for EV-linked miRNAs in two batches and in our subsequent statistical analyses we controlled for batch (batch 1 vs batch 2).

Statistical Analysis:

Descriptive statistics and normalization of EV-linked miRNAs: Thermo Fisher Cloud Relative Quantification software was used to extract the EV-linked miRNA qPCR data. To ensure accuracy of in our normalization methods of the EV-linked miRNAs, we ran algorithms to identify the best normalization strategy. We first applied the NormFinder and geNorm algorithms to select the best normalization strategy among global mean (arithmetic and geometric), RNU48, RNU6, or the average of the four miRNAs with the lowest standard deviation (SD) among subjects. Based on these algorithms, we found that global mean was the best method to normalize the data. EV-linked miRNAs data was normalized using the global mean (GM) method ($\Delta C_{rt\_EV\text{-}linked\ miRNAi} = (C_{rt\_EV\text{-}linked\ miRNAi} - C_{rt\_EV\text{-}linked\ miRNAi\_global\_mean})$) (38). All the EV-linked miRNA with a Crt value > 28 and/or an amplification score ≤ 1.24 were identified as unexpressed. For the global mean, we coded all those EV-linked miRNAs that were unexpressed as 28 as suggested by Pergoli et al. (41). We calculated the delta Crt based on the global mean across all the miRNAs within that subject and dividing it by the total miRNAs (N=754). All subsequent analyses were performed exclusively on those EV-linked miRNAs that had expressed values, which were detected in at least 15% of our samples, based on the histogram distribution of the percent detected in our samples (Supplemental Figure S1). This cut-off was chosen to maximize the number of EV-linked miRNAs examined while retaining a large enough sample to assess the associations (at least 20 individuals), while removing those EV-linked miRNAs that had a very large missing rate. Standard descriptive statistics were used to explore the characteristics of the study participants and exposure data. Spearman's correlation coefficients were used to examine correlations between covariates and exposure variables.

EV-linked miRNA-by-EV-linked miRNA Regression Analysis: Linear regression models were performed to elucidate top hit EV-linked miRNAs. Models were adjusted for continuous age (years), continuous BMI, categorical smoking status, binary race/nationality, binary batch, and continuous SVA surrogate variables, identified by the SVA package in R. The SVA package can help identify and remove any batch effects or unwanted sources of variation, seasonal, meteorological, exposure, or technical variables, which are unknown but might be differently distributed in the two batches of samples. It creates surrogate variables,

accounting for the unmeasured variation, that act as covariates in our models that would account for any unknown, un-modeled, or other sources of (42, 43). EV-linked miRNA outcomes were inverse normally transformed to ensure normality with a standard deviation of 1. To account for multiple-testing, we applied the Benjamini-Hochberg FDR "p.adjust" function in R (44). All statistical analyses were performed in R-version 3.4.0 (45). Statistical significance was set at a p-value < 0.05. We used the Benjamini-Hochberg False-Discovery Rate (FDR) (44) to account for multiple testing and chose a threshold, FDR q-value < 0.05.

Principal Component Analysis: Principal component analyses (PCA) were performed to examine the overall variation of EV-linked miRNA profiles. All of the selected 192 EV-linked miRNAs were included in the analysis. The function "prcomp" in R was used to calculate the principal components (PCs) and the PC loadings for each component. All variables were scaled and centered with a mean of 0 and a standard deviation of 1 prior to the PCA. PCs were inverse normally transformed for normality. Separate unadjusted univariate analyses were performed on age, smoking status, and BMI using linear regression with each principal component as the outcome. Mutually adjusted linear regressions were performed with the principal components as the outcomes and adjusted for age, BMI, smoking status, race, batch, and SVA surrogate variables. Absolute values of the PC loadings were taken and the EV-linked miRNAs that contributed a loading in the 90th percentile or higher were examined further. This threshold was chosen based on both the histogram distribution of the absolute values of the PC loadings (Supplemental Figure S3) and the percentile cutoffs (Supplemental Table S5). This would allow us to examine those EV-linked miRNAs that are the most important to the principal component while keeping the number of EV-linked miRNAs manageable.

Kyoto Encyclopedia of Genes and Genomes (KEGG) Pathway Analysis:

An *in-silico* analysis using a web-based tool, miRWalk2.0 (http://mirwalk.umm.uni-heidelberg.de/) was performed to investigate gene targets of EV-linked miRNAs (46). Target predictions included a comparative analysis of seven prediction programs: DIANAmT, miRanda, miRDB, miRWalk, PICTAR5, RNA22, and Targetscan. To decrease the number of false positive pathways, targeted genes were identified that were validated in a total of five prediction programs including Targetscan and any combination of at least four of the other prediction programs. The predicted target search examined promoter, 5'-untranslated regions, 3'-untranslated regions, and coding sequences and included a minimum seed length of 7 nucleotides (46). Using the genes selected by miRWalk, we ran a Kyoto Encyclopedia of Genes and Genomes (KEGG) pathway enrichment analysis using the web-based tool DAVID (https://david.ncifcrf.gov/summary.jsp) (47, 48). We restricted our results to only those with 10 or more genes listed in the *in silico* predicted targets and an FDR q-value < 0.05.

Results:

Study Population

This study consisted of 133 women, mainly Caucasians (92%), while the other 8% consisted of women from other ethnicities (Asian, African, and Hispanic). On average, the women in

our study were 30.9 ± 3.7 years of age (mean ± standard deviation), had a BMI of 23.6 ± 4.7 kg/m^2, and 9.4 ± 5.1 oocytes retrieved during the IVF cycle (Table 1). The majority of women were never smokers (54%) and 26% were current smokers. Most of the women were attempting IVF for the first time (65%).

Profile of EV-linked miRNAs in follicular fluid

We screened for EV-linked miRNAs from a panel of 754 microRNAs in follicular fluid samples collected from follicles that contained mature oocytes. We detected a signal for 320 EV-linked miRNAs in at least one of the 133 follicular fluid samples analyzed. Of these, 192 EV-linked miRNAs met our pre-determined threshold for inclusion and were therefore considered as expressed. A list of the selected EV-linked miRNAs with their percent expression levels are provided in Supplemental Table S1.

Associations between Body Mass Index and EV-linked miRNA expression in follicular fluid

Possible associations between follicular fluid EV-linked miRNAs and BMI were investigated using regression for each EV-linked miRNA. Models adjusted for age, smoking status, race, batch, and SVA surrogate variables and modeled BMI continuously. Eighteen EV-linked miRNAs were marginally significantly associated with BMI ($p < 0.05$) (Table 2 and Supplemental Table S2) and after adjusting for multiple testing, hsa-miR-328 remained significant. A one unit increase in BMI was associated with an increase of hsa-miR-328 expression value (ΔCt) in 0.03 standard deviation [95% CI: 0.02, 0.05; q-value: 0.03].

Using PCA to examine global variability of EV-linked miRNA profile

Global variability of EV-linked miRNAs was explored using PCA, which revealed that the first three PCs explained over 50% of the variability in the outcome data set (PC1: 40%, PC2: 6%, PC3: 5%) (Supplemental Figure S2). No associations were identified between smoking status, BMI, and age with these PCs in unadjusted univariate analyses; however, mutually adjusted models identified PC1 to be significantly associated with BMI (p-value: 0.01) (Supplemental Table S3). This association remained significant after FDR (q-value: 0.04). To further examine the makeup of PC1, the absolute values of the PC loadings were examined (Supplemental Figure S3 and Supplemental Table S4). Twenty-five EV-linked miRNAs in PC1 with a PC loading in the 90^{th} percentile or higher (90^{th} percentile threshold > 0.10) were identified. Six EV-linked miRNAs were identified in both the top 25 EV-linked miRNAs from PC1 and the 18 top EV-linked miRNAs from the BMI analyses (Figure 2).

In Silico KEGG Pathways analyses

KEGG Pathways of EV-linked miRNAs associated with BMI—We performed two KEGG analysis with these EV-linked miRNAs associated with BMI. The first examined the 18 EV-linked miRNAs that were associated with BMI in the EV-linked miRNA-by-EV-linked miRNA analysis. For this analysis, the miRWalk tool recognized 1872 unique genes that were predicted from at least four prediction programs and the TargetScan software. The DAVID software identified 18 FDR significant KEGG pathways that were associated with unique genes related to these EV-linked miRNAs. Twelve of these identified KEGG pathways are related to oocyte and follicle development and maturation (Figure 1).

The second BMI KEGG analysis examined the 25 EV-linked miRNAs having a PC loading in the 90th percentile or above in PC1. The miRWalk software recognized 4092 unique genes and the DAVID software found 43 KEGG pathways significantly associated with these 4092 genes (q-value < 0.05). Among these 43 KEGG pathways, 24 were involved with biological processes of interest to our study (Figure 1).

Discussion:

In the present study, we identified 18 EV-linked miRNAs associated with BMI. Of those, only hsa-miR-328 remained statistically significant after FDR-adjustment. Additionally, principal component analysis was applied to examine the global variability in the profile of 192 EV-linked miRNAs. The first principal component explained 40% of the variability in the EV-linked miRNA dataset and was significantly associated with an increased BMI in a mutually adjusted model.

It has been well established that an increased BMI is associated with decreased fertility outcomes, such as reduced pregnancy and fertilization rates (10-12, 49). We found hsa-miR-328 was significantly associated with BMI after adjusting for covariates and taking into account multiple testing. Further examination of hsa-miR-328 identified associations with cancer (50, 51). MiR-328 has been known to play a role in myocardial infarction and cancers in adults, where obesity is an established risk factor (52). A study examining childhood obesity and circulating miRNAs found circulating concentrations of hsa-miR-328 were higher in obese compared to lean children (53). This suggests that hsa-miR-328 might play a role in adipose regulation, obesity, and obesity related diseases. A rodent study found that reducing expression of miR-328 blocked pre-adipocyte commitment and inducing miR-328 instigated differentiation of brown adipose tissue (54).

Few studies have examined the underlying molecular mechanisms linking BMI with fertility. One previous study assessed the associations between circulating plasma microRNAs and BMI and found 19 significant microRNAs, including hsa-miR-193b-3p (55). This was the only overlapping EV-linked miRNA with our analysis, but the directionality of the association with hsa-miR-193b-3p was the opposite of that previously reported (55). Another study examined pre-pregnancy BMI and circulating miRNAs during pregnancy and identified 27 significant miRNAs in two separate cohorts. Specifically, hsa-miR-28-5p, hsa-miR-376a, has-miR-139-5p, and hsa-miR-423-5p were found to overlap with those EV-linked miRNAs which were significantly associated with BMI in our analysis (56). Even more EV-linked miRNAs overlapped with Enquobahrie et al, however, the direction of association was not consistent for hsa-miR-376a and hsa-miR-139-5p (56).

We also examined whether the global variability of EV-linked miRNAs were associated with BMI. EV-linked miRNAs can come from different non-coding sequences but can target the same messenger RNA transcripts (57). Thus, one EV-linked miRNA can interfere with the expression of many genes and that one gene can be negatively regulated or silenced by many EV-linked miRNAs. Our PCA identified principal components that would explain a certain percentage of the variability within our EV-linked miRNA dataset and found PC1 was significantly associated with BMI. This suggests that the biological variability captured by

PC1 was significantly associated with BMI. From these two analyses, six EV-linked miRNAs overlapped as significant, hsa-miR-99b, hsa-miR-29a, hsa-miR-28, hsa-miR-328, hsa-miR-152, and hsa-miR-331. The EV-linked miRNA that was FDR significant in the EV-linked miRNA by EV-linked miRNA analysis, hsa-miR-328, was identified as significant in both analyses. This suggests that this hsa-miR-328 might be an important EV-linked miRNA that could be impacted by an increase in BMI.

Our KEGG pathway analysis of the top EV-linked miRNAs contributing to PC1 revealed several pathways associated with pathways of cellular signaling, follicular growth, oocyte maturation (58-62). We also performed KEGG pathway analyses on the 18 EV-linked miRNAs associated with BMI in the EV-linked miRNA-by-EV-linked miRNA regression analyses. We identified 16 significant pathways that overlapped between the three KEGG analyses. Eleven of these were associated with oocyte and follicle maturation and development: ECM-receptor interaction, focal adhesion, FoxO signaling, oocyte meiosis, PI3K-Akt signaling, adipocytokine signaling, AMPK signaling, cGMP-PKG signaling, ErbB signaling, gap junction, and GnRH signaling pathways.

These 11 aforementioned pathways contribute to oocyte development, maturation, and signaling. More notably the Pl3K-Akt pathway has been associated with recruitment of primordial follicles, granulosa proliferation, and ovarian function (63). It also activates the mTOR and FoxO pathways (64). The FoxO pathway plays an important role in intra-oocyte signaling and can negatively regulate oocyte growth and follicular development by acting as a regulatory switch to initiate primordial follicle activation (65-68). The pathway of oocyte maturation is induced to transform an immature oocyte into a mature or fertilizable egg (69). ECM-receptor interaction (extracellular matrix) is believed to play an essential role in regulating follicle development (70) and significantly contributes to follicle microenvironments that allow intracellular communication to occur between cells and the oocyte (70). Focal adhesion is necessary to establish or maintain the oocyte-granulosa cell contact in the follicle (71). Pathways identified by the significant EV-linked miRNAs play major roles in follicle and oocyte development and maturation, suggesting that BMI could disrupt these processes. This could provide a mechanistic explanation for the reduced fertility rates and increased spontaneous abortion rates that are observed with an increased BMI.

This study has limitations. First, we quantified EV-linked miRNA profiles from a single follicle, it might not accurately represent the EV-linked miRNA profile of the whole cohort of follicles. In a previous analysis (unpublished data) we compared the profile of EV-linked miRNA from two follicles per patients that contained mature oocytes, and their profiles were highly correlated. As the single follicle did not always contain the oocyte that yielded the embryo that was transferred and in many of the cases more than one embryo was transferred, we were limited in testing associations of BMI, EV-linked BMI and pregnancy outcomes. Second, we ran our KEGG pathway analyses on a relatively small number of EV-linked miRNAs. Thus, our results may be subject to overfitting of the selected pathways by the software. To minimize this, we set our inclusion of genes to those found in at least four separate prediction software packages in addition to the Target scan database. We also included those EV-linked miRNAs that were marginally significant but did not meet the

FDR threshold for multiple comparisons. EV-linked miRNAs are highly correlated and have high biological variability between samples, so to prioritize biological relevance in our pathway analyses we chose to include all those EV-linked miRNAs that met the marginally significant threshold ($p < 0.05$). In addition, while we can assure that we have a pellet enriched in EVs, it is possible that the pellet included not only miRNAs that are encapsulated within the EV, but also miRNAs that were extracellularly attached to EVs (28). Additionally, there is a possibility that some of the miRNAs in the pellet derived either from necrotic cells (28, 72). To ensure we extract EV-linked miRNAs, we have optimized our protocol by running thousands of samples in previous large studies investigating EV-linked miRNAs as well as assessed random follicular fluid samples by Nanosight and flow cytometry.

Our study has significant strengths as well. First, to our knowledge, this is the first study to examine BMI with respect to EV-linked miRNAs in follicular fluid. Second, we used PCA to examine how EV-linked miRNAs contribute to variability in our dataset, allowing us not only to expand upon work done by others, but also to examine the global variability of the outcomes.

In conclusion, these identified associations between an increased BMI and follicular fluid EV-linked miRNAs may provide an insight as to how higher BMI may disrupt fertility on a mechanistic level.

Supplementary Material

Refer to Web version on PubMed Central for supplementary material.

Acknowledgements:

This work was supported by the National Institutes of Environmental Health Sciences [Grant R21-ES024236]; Israeli Science Foundation [Grant 1936/12]; the Environmental Health Fund, Israel [Grant 1301]; and Education and Research Center for Occupational Safety and Health CDC/NIOSH [grant award T42/OH008416]

References

1. Mascarenhas MN, Flaxman SR, Boerma T, Vanderpoel S, Stevens GA. National, Regional, and Global Trends in Infertility Prevalence Since 1990: A Systematic Analysis of 277 Health Surveys. PLOS Medicine 2012;9:e1001356. [PubMed: 23271957]
2. Rossi BV, Abusief M, Missmer SA. Modifiable Risk Factors and Infertility: What are the Connections? Am J Lifestyle Med 2014;10:220–31. [PubMed: 27594813]
3. Klonoff-Cohen H Female and male lifestyle habits and IVF: what is known and unknown. Human reproduction update 2005;11:179–203. [PubMed: 15708968]
4. Hornstein MD. Lifestyle and IVF Outcomes. Reproductive sciences (Thousand Oaks, Calif) 2016;23:1626–9.
5. Frattarelli JL, Kodama CL. Impact of Body Mass Index on In Vitro Fertilization Outcomes. J Assist Reprod Genet 2004;21:211–5. [PubMed: 15526976]
6. Jungheim ES, Macones GA, Odem RR, Patterson BW, Lanzendorf SE, Ratts VS et al. Associations between free fatty acids, cumulus oocyte complex morphology and ovarian function during in vitro fertilization. Fertil Steril 2011;95:1970–4. [PubMed: 21353671]

7. Matalliotakis I, Cakmak H, Sakkas D, Mahutte N, Koumantakis G, Arici A. Impact of body mass index on IVF and ICSI outcome: a retrospective study. Reproductive biomedicine online 2008;16:778–83. [PubMed: 18549686]
8. Robker RL. Evidence that obesity alters the quality of oocytes and embryos. Pathophysiology : the official journal of the International Society for Pathophysiology 2008;15:115–21. [PubMed: 18599275]
9. Esinler I, Bozdag G, Yarali H. Impact of isolated obesity on ICSI outcome. Reproductive biomedicine online 2008;17:583–7. [PubMed: 18854116]
10. Petanovski Z, Dimitrov G, Ajdin B, Hadzi-Lega M, Sotirovska V, Matevski V et al. Impact of body mass index (BMI) and age on the outcome of the IVF process. Prilozi 2011;32:155–71. [PubMed: 21822185]
11. Lintsen AM, Pasker-de Jong PC, de Boer EJ, Burger CW, Jansen CA, Braat DD et al. Effects of subfertility cause, smoking and body weight on the success rate of IVF. Human reproduction (Oxford, England) 2005;20:1867–75.
12. Bellver J, Ayllon Y, Ferrando M, Melo M, Goyri E, Pellicer A et al. Female obesity impairs in vitro fertilization outcome without affecting embryo quality. Fertil Steril 2010;93:447–54. [PubMed: 19171335]
13. Rimon-Dahari N, Yerushalmi-Heinemann L, Alyagor L, Dekel N. Ovarian Folliculogenesis In: Piprek RP, ed. Molecular Mechanisms of Cell Differentiation in Gonad Development. Cham: Springer International Publishing, 2016:167–90.
14. Hennet ML, Combelles CM. The antral follicle: a microenvironment for oocyte differentiation. The International journal of developmental biology 2012;56:819–31. [PubMed: 23417404]
15. Machtinger R, Laurent LC, Baccarelli AA. Extracellular vesicles: roles in gamete maturation, fertilization and embryo implantation. Human reproduction update 2016;22:182–93. [PubMed: 26663221]
16. Fortune JE. Ovarian follicular growth and development in mammals. Biology of reproduction 1994;50:225–32. [PubMed: 8142540]
17. Scalici E, Traver S, Molinari N, Mullet T, Monforte M, Vintejoux E et al. Cell-free DNA in human follicular fluid as a biomarker of embryo quality. Hum Reprod 2014;29:2661–9. [PubMed: 25267787]
18. Baka S, Malamitsi-Puchner A. Novel follicular fluid factors influencing oocyte developmental potential in IVF: a review. Reproductive biomedicine online 2006;12:500–6. [PubMed: 16740225]
19. De Placido G, Alviggi C, Clarizia R, Mollo A, Alviggi E, Strina I et al. Intra-follicular leptin concentration as a predictive factor for in vitro oocyte fertilization in assisted reproductive techniques. J Endocrinol Invest 2006;29:719–26. [PubMed: 17033261]
20. Revelli A, Piane LD, Casano S, Molinari E, Massobrio M, Rinaudo P. Follicular fluid content and oocyte quality: from single biochemical markers to metabolomics. Reprod Biol Endocrinol 2009;7:40. [PubMed: 19413899]
21. Machtinger R, Rodosthenous RS, Adir M, Mansour A, Racowsky C, Baccarelli AA et al. Extracellular microRNAs in follicular fluid and their potential association with oocyte fertilization and embryo quality: an exploratory study. J Assist Reprod Genet 2017;34:525–33. [PubMed: 28188594]
22. Weber JA, Baxter DH, Zhang S, Huang DY, How Huang K, Jen Lee M et al. The MicroRNA Spectrum in 12 Body Fluids. Clin Chem 2010;56:1733–41. [PubMed: 20847327]
23. Tannetta D, Dragovic R, Alyahyaei Z, Southcombe J. Extracellular vesicles and reproduction-promotion of successful pregnancy. Cell Mol Immunol 2014;11:548–63. [PubMed: 24954226]
24. Lim LP, Lau NC, Garrett-Engele P, Grimson A, Schelter JM, Castle J et al. Microarray analysis shows that some microRNAs downregulate large numbers of target mRNAs. Nature 2005;433:769. [PubMed: 15685193]
25. Li SC, Tang P, Lin WC. Intronic microRNA: discovery and biological implications. DNA and cell biology 2007;26:195–207. [PubMed: 17465886]
26. Sætrom P, Snøve O Jr, Rossi JJ. Epigenetics and MicroRNAs. Pediatr Res 2007;61:17R.
27. Raposo G, Stoorvogel W. Extracellular vesicles: exosomes, microvesicles, and friends. The Journal of cell biology 2013;200:373–83. [PubMed: 23420871]

28. Hill AF, Pegtel DM, Lambertz U, Leonardi T, O'Driscoll L, Pluchino S et al. ISEV position paper: extracellular vesicle RNA analysis and bioinformatics. J Extracell Vesicles 2013;2:10.3402/jev.v2i0.22859.
29. Di Pietro C Exosome-mediated communication in the ovarian follicle. J Assist Reprod Genet 2016;33:303–11. [PubMed: 26814471]
30. Yáñez-Mó M, Siljander PRM, Andreu Z, Bedina Zavec A, Borrás FE, Buzas EI et al. Biological properties of extracellular vesicles and their physiological functions. J Extracell Vesicles 2015;4:27066. [PubMed: 25979354]
31. Ferrante SC, Nadler EP, Pillai DK, Hubal MJ, Wang Z, Wang JM et al. Adipocyte-derived Exosomal miRNAs: A Novel Mechanism for Obesity-Related Disease. Pediatr Res 2015;77:447–54. [PubMed: 25518011]
32. Bollati V, Iodice S, Favero C, Angelici L, Albetti B, Cacace R et al. Susceptibility to particle health effects, miRNA and exosomes: rationale and study protocol of the SPHERE study. BMC Public Health 2014;14:1137. [PubMed: 25371091]
33. Shi X-F, Wang H, Kong F-X, Xu Q-Q, Xiao F-J, Yang Y-F et al. Exosomal miR-486 regulates hypoxia-induced erythroid differentiation of erythroleukemia cells through targeting Sirt1. Exp Cell Res 2017;351:74–81. [PubMed: 28043832]
34. Jones A, Danielson KM, Benton MC, Ziegler O, Shah R, Stubbs RS et al. miRNA signatures of insulin resistance in obesity. Obesity (Silver Spring, Md) 2017;25:1734–44.
35. World Medical Association Declaration of Helsinki: ethical principles for medical research involving human subjects. Jama 2013;310:2191–4. [PubMed: 24141714]
36. Ferraretti AP, La Marca A, Fauser BC, Tarlatzis B, Nargund G, Gianaroli L et al. ESHRE consensus on the definition of 'poor response' to ovarian stimulation for in vitro fertilization: the Bologna criteria. Human reproduction (Oxford, England) 2011;26:1616–24.
37. Witwer KW, Buzas EI, Bemis LT, Bora A, Lasser C, Lotvall J et al. Standardization of sample collection, isolation and analysis methods in extracellular vesicle research. J Extracell Vesicles 2013;2.
38. Pergoli L, Cantone L, Favero C, Angelici L, Iodice S, Pinatel E et al. Extracellular vesicle-packaged miRNA release after short-term exposure to particulate matter is associated with increased coagulation. Part Fibre Toxicol 2017;14:32. [PubMed: 28899404]
39. Gardiner C, Di Vizio D, Sahoo S, Thery C, Witwer KW, Wauben M et al. Techniques used for the isolation and characterization of extracellular vesicles: results of a worldwide survey. J Extracell Vesicles 2016;5:32945. [PubMed: 27802845]
40. Enderle D, Spiel A, Coticchia CM, Berghoff E, Mueller R, Schlumpberger M et al. Characterization of RNA from Exosomes and Other Extracellular Vesicles Isolated by a Novel Spin Column-Based Method. PloS one 2015;10:e0136133. [PubMed: 26317354]
41. Pergoli L, Cantone L, Favero C, Angelici L, Iodice S, Pinatel E et al. Extracellular vesicle-packaged miRNA release after short-term exposure to particulate matter is associated with increased coagulation. Particle and fibre toxicology 2017;14:32. [PubMed: 28899404]
42. Leek JT, Johnson WE, Parker HS, Jaffe AE, Storey JD. The sva package for removing batch effects and other unwanted variation in high-throughput experiments. Bioinformatics 2012;28:882–3. [PubMed: 22257669]
43. Jeffery T Leek WEJ, Parker Hilary S., Fertig Elana J., Jaffe Andrew E., Storey John D., Zhang Yuqing, and Torres Leonardo Collado. sva: Surrogate Variable Analysis. In. Vol. package version 3.24.4: R, 2017.
44. Benjamini Y, Hochberg Y. Controlling the False Discovery Rate: A Practical and Powerful Approach to Multiple Testing. J R Stat Soc Series B Stat [Methodol] 1995;57:289–300.
45. R-Core-Team. R: A language and environment for statistical computing. In. Vienna, Austria: R Foundation for Statistical Computing, 2017.
46. Dweep H, Sticht C, Pandey P, Gretz N. miRWalk – Database: Prediction of possible miRNA binding sites by “walking” the genes of three genomes. J Biomed Inform 2011;44:839–47. [PubMed: 21605702]
47. Huang DW, Sherman BT, Lempicki RA. Systematic and integrative analysis of large gene lists using DAVID bioinformatics resources. Nat Proto 2008;4:44.

48. Huang DW, Sherman BT, Lempicki RA. Bioinformatics enrichment tools: paths toward the comprehensive functional analysis of large gene lists. Nucleic Acids Res 2009;37:1–13. [PubMed: 19033363]
49. Lintsen AME, on behalf of the Opg, Pasker-de Jong PCM, on behalf of the Opg, de Boer EJ, on behalf of the Opg et al. Effects of subfertility cause, smoking and body weight on the success rate of IVF. Hum Reprod 2005;20:1867–75. [PubMed: 15817580]
50. Wu Z, Sun L, Wang H, Yao J, Jiang C, Xu W et al. MiR-328 Expression Is Decreased in High-Grade Gliomas and Is Associated with Worse Survival in Primary Glioblastoma. PloS one 2012;7:e47270. [PubMed: 23077581]
51. Ishimoto T, Sugihara H, Watanabe M, Sawayama H, Iwatsuki M, Baba Y et al. Macrophage-derived reactive oxygen species suppress miR-328 targeting CD44 in cancer cells and promote redox adaptation. Carcinogenesis 2014;35:1003–11. [PubMed: 24318997]
52. Brettfeld C, Maver A, Aumuller E, Peterlin B, Haslberger AG. MicroRNAs Responsible for Inflammation in Obesity, 2017.
53. Prats-Puig A, Ortega FJ, Mercader JM, Moreno-Navarrete JM, Moreno M, Bonet N et al. Changes in Circulating MicroRNAs Are Associated With Childhood Obesity. J Clin Endocrinol Metab 2013;98:E1655–E60. [PubMed: 23928666]
54. Oliverio M, Schmidt E, Mauer J, Baitzel C, Hansmeier N, Khani S et al. Dicer1-miR-328-Bace1 signalling controls brown adipose tissue differentiation and function. Nature cell biology 2016;18:328–36. [PubMed: 26900752]
55. Ameling S, Kacprowski T, Chilukoti RK, Malsch C, Liebscher V, Suhre K et al. Associations of circulating plasma microRNAs with age, body mass index and sex in a population-based study. BMC Med Genom 2015;8:61.
56. Enquobahrie DA, Wander PL, Tadesse MG, Qiu C, Holzman C, Williams MA. Maternal pre-pregnancy body mass index and circulating microRNAs in pregnancy. Obes Res Clin Pract 2017;11:464–74. [PubMed: 27789200]
57. Bartel DP. MicroRNA Target Recognition and Regulatory Functions. Cell 2009;136:215–33. [PubMed: 19167326]
58. Knight PG, Glister C. Local roles of TGF-beta superfamily members in the control of ovarian follicle development. Animal reproduction science 2003;78:165–83. [PubMed: 12818643]
59. Boyer A, Goff AK, Boerboom D. WNT signaling in ovarian follicle biology and tumorigenesis. Trends in endocrinology and metabolism: TEM 2010;21:25–32. [PubMed: 19875303]
60. Boerboom D, Paquet M, Hsieh M, Liu J, Jamin SP, Behringer RR et al. Misregulated Wnt/beta-catenin signaling leads to ovarian granulosa cell tumor development. Cancer research 2005;65:9206–15. [PubMed: 16230381]
61. Zhang M, Ouyang H, Xia G. The signal pathway of gonadotrophins-induced mammalian oocyte meiotic resumption. Molecular human reproduction 2009;15:399–409. [PubMed: 19443606]
62. Conti M, Hsieh M, Zamah AM, Oh JS. Novel signaling mechanisms in the ovary during oocyte maturation and ovulation. Molecular and cellular endocrinology 2012;356:65–73. [PubMed: 22101318]
63. Andrade GM, da Silveira JC, Perrini C, Del Collado M, Gebremedhn S, Tesfaye D et al. The role of the PI3K-Akt signaling pathway in the developmental competence of bovine oocytes. PloS one 2017;12:e0185045. [PubMed: 28922408]
64. Makker A, Goel MM, Mahdi AA. PI3K/PTEN/Akt and TSC/mTOR signaling pathways, ovarian dysfunction, and infertility: an update. J Mol Endocrinol 2014;53:R103–R18. [PubMed: 25312969]
65. Liu L, Rajareddy S, Reddy P, Du C, Jagarlamudi K, Shen Y et al. Infertility caused by retardation of follicular development in mice with oocyte-specific expression of Foxo3a. Development (Cambridge, England) 2007;134:199–209.
66. Pelosi E, Omari S, Michel M, Ding J, Amano T, Forabosco A et al. Constitutively Active Foxo3 in Oocytes Preserves Ovarian Reserve in Mice. Nat Commun 2013;4:1843. [PubMed: 23673628]
67. Brenkman AB, Burgering BM. FoxO3a eggs on fertility and aging. Trends in molecular medicine 2003;9:464–7. [PubMed: 14604822]

68. John GB, Gallardo TD, Shirley LJ, Castrillon DH. Foxo3 is a PI3K-dependent molecular switch controlling the initiation of oocyte growth. Developmental biology 2008;321:197–204. [PubMed: 18601916]

69. Schmitt A, Nebreda AR. Signalling pathways in oocyte meiotic maturation. J Cell Sci 2002;115:2457. [PubMed: 12045215]

70. Woodruff TK, Shea LD. The Role of the Extracellular Matrix in Ovarian Follicle Development. Reproductive sciences (Thousand Oaks, Calif) 2007;14:6–10.

71. McGinnis LK, Kinsey WH. Role of focal adhesion kinase in oocyte-follicle communication. Mol Reprod Dev 2015;82:90–102. [PubMed: 25536210]

72. Endzelins E, Berger A, Melne V, Bajo-Santos C, Sobolevska K, Abols A et al. Detection of circulating miRNAs: comparative analysis of extracellular vesicle-incorporated miRNAs and cell-free miRNAs in whole plasma of prostate cancer patients. BMC cancer 2017;17:730. [PubMed: 29121858]

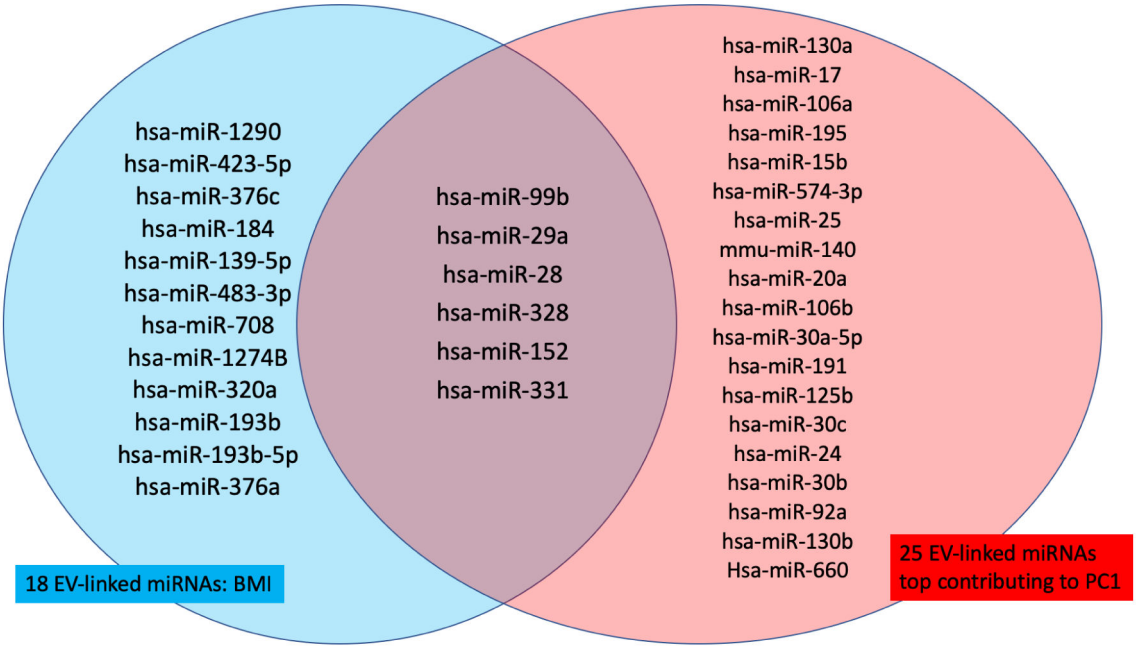

Figure 1. Venn diagram of EV-linked miRNAs identified in linear models and PCA.

Venn diagram of EV-linked miRNAs identified in the linear regression models and principal component analysis. Red EV-linked miRNAs represent the top identified EV-linked miRNAs associated with the 90th percentile of PC1 loadings. Blue EV-linked miRNAs represent those EV-linked miRNAs that were found to be marginally significant in linear models ($p < 0.05$).

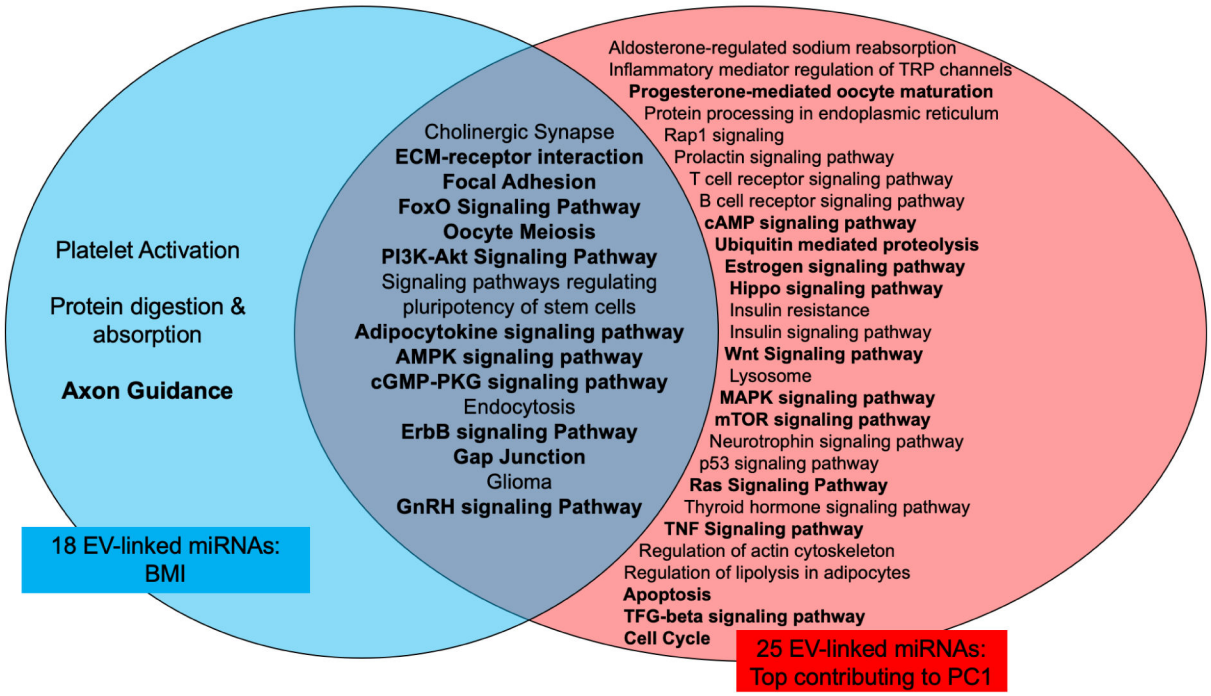

Figure 2. Venn diagram of FDR significant KEGG pathways.

Venn diagram of FDR significant KEGG pathways identified from KEGG analyses. Red pathways represent those KEGG pathways identified with EV-linked miRNAs associated with the 90th percentile of PC1 loadings. Blue pathways represent those KEGG pathways that were associated with EV-linked miRNAs and BMI. Bolded pathways indicate a KEGG pathway associated with oocyte or follicle maturation, development, or fertilization.

Table 1.

Patients' demographic characters (N= 133)

Age, years		30.9 ± 3.7
BMI, kg/m^2		23.6 ± 4.7
Number of oocytes retrieved		9.4 ± 5.1
WHO BMI categories	Underweight	15 (11%)
	Normal	73 (56%)
	Overweight	31 (23%)
	Obese	14 (10%)
Smoking Status	Never Smoker	72 (54%)
	Ever Smoker	27 (20%)
	Current Smoker	34 (26%)
IVF attempts	First IVF Attempt	87 (65%)
	IVF Attempt > 1	46 (35%)
Ethnicity	Caucasian	122 (92%)
	Asian	8 (6%)
	African	1 (1%)
	Hispanic	2 (1%)
Diagnosis	PGD	57 (43%)
	Male Factor	53 (40%)
	Unexplained	20 (15%)
	Other[a]	3 (2%)
Pre-IVF Fertility Status	Fertile	58 (44%)
	Infertile	75 (56%)

Values represent: mean ± SD or number (%)

Abbreviations: BMI - Body mass index, SD - Standard Deviation, IVF - In Vitro Fertilization, PGD - Pre-gestational diagnosis

Table 2.

P-value significant EV-linked miRNAs associated with Body Mass Index and Top FDR Significant EV-linked miRNA [c]

EV-linked miRNA Name	% Expressed in Population (# of samples)	Effect Size [b]	95% Confidence Interval	Unadjusted p-value	FDR q-value [a]
hsa-miR-328 **	100% (n = 133)	0.032	[0.016, 0.048]	< 0.001	0.03
hsa-miR-1290	51% (n = 67)	0.049	[0.016, 0.081]	0.004	0.3
hsa-miR-193b-3p	100% (n = 133)	0.03	[0.008, 0.051]	0.01	0.3
hsa-miR-193b-5p	52% (n = 69)	0.035	[0.009 0.061]	0.01	0.3
hsa-miR-29a	93% (n = 123)	0.018	[0.005, 0.032]	0.01	0.3
hsa-miR-99b	100% (n = 133)	0.017	[0.004, 0.031]	0.01	0.3
hsa-miR-331	100% (n = 133)	0.017	[0.004, 0.031]	0.01	0.3
hsa-miR-423-5p	69% (n = 91)	0.028	[0.005, 0.052]	0.02	0.39
hsa-miR-320a	100% (n = 133)	0.022	[0.003, 0.040]	0.02	0.46
hsa-miR-720	98% (n = 130)	0.028	[0.003, 0.054]	0.03	0.5
hsa-miR-28	99% (n = 131)	0.017	[0.001, 0.032]	0.03	0.5
hsa-miR-483-5p	100% (n = 133)	0.027	[0.002, 0.052]	0.03	0.5
hsa-miR-152	89% (n = 118)	0.018	[0.001, 0.035]	0.03	0.5
hsa-miR-376a	95% (n = 126)	−0.023	[−0.045, −0.001]	0.04	0.5
hsa-miR-376c	84% (n = 111)	−0.023	[−0.046, −0.001]	0.04	0.5
hsa-miR-1274B	100% (n = 133)	0.026	[0.001, 0.051]	0.04	0.5
hsa-miR-184	53% (n = 70)	0.023	[0.000, 0.047]	0.05	0.51
hsa-miR-139-5p	71% (n = 94)	−0.024	[−0.049, 0.000]	0.05	0.51

** FDR significant EV-linked miRNA, after adjusting for multiple testing

[a] FDR q-value adjusted for multiple testing for the 192 EV-linked miRNAs

[b] For every one unit increase in BMI, there is an effect size increase/decrease in standard deviation of EV-linked miRNA ΔCt, with a lower ΔCt indicates higher expression

[c] Models were adjusting for age, smoking status, ethnicity, batch, and SVA surrogate variables